NANJING INSTITUTE OF GEOPHYSICAL PROSPECTING AND INSTITUTE OF PHYSICS PUBLISHING JOURNAL OF GEOPHYSICS AND ENGINEERING

J. Geophys. Eng. **3** (2006) 43–49 doi:10.1088/1742-2132/3/1/006

Remotely sensing the thickness of the Bushveld Complex UG2 platinum reef using borehole radar

C M Simmat[1], P Le R Herselman[2], M Rütschlin[2], I M Mason[1] and J H Cloete[1]

[1] Geophysical Imaging Lab, School of Geosciences, University of Sydney, NSW, 2006, Australia
[2] Department of Electrical and Electronic Engineering, University of Stellenbosch, Private Bag X1, Stellenbosch, 7602, South Africa

E-mail: carina@geosci.usyd.edu.au

Received 4 October 2005
Accepted for publication 12 January 2006
Published 7 February 2006
Online at stacks.iop.org/JGE/3/43

Abstract
The planar, 80 cm thick, lossy dielectric reefs of the Bushveld are embedded in rocks that are almost transparent at ground penetrating radar frequencies of 10–125 MHz. Pothole sensing practices are based largely on using borehole radars to observe departures of the reefs from planarity. Surveys are run in ∼200 m near-horizontal boreholes that are drilled into the footwalls of the reef. Careful laboratory measurements of the Jonscher dielectric parameters of the stratigraphic column through the UG2 reef are translated by electro-dynamic modelling into a prediction that platinum reef thinning can be sensed remotely by footwall borehole radars. This proposition sheds light on the results of a recent borehole radar survey that was shot in ∼180 m long AXT (48 mm diameter) boreholes. Areas of sub-economical UG2 thickness (typically less than ∼50 cm) were mapped by studying the relative amplitudes of echoes from the reef and a pyroxenite–anorthosite interface in its hanging wall, with the radar deployed beneath the UG2 in its footwall.

Keywords: VHF borehole radar, electro-dynamic modelling, remote sensing, mine planning, platinum reef thickness

Introduction

The 2060 Ma old Bushveld Complex is a massive layered igneous intrusion, with outcrop extremities of ∼450 km east–west and ∼300 km north–south. It has been variously attributed to the subduction of a mid-oceanic spreading centre, a multiple meteorite impact, and a mantle plume (Cawthorn 1999). Geometrically it can be compared to an enormous, irregularly shaped saucer with its centre deeply buried, and its rim exposed. The saucer itself is made up of distinct layers, two of which, the Merensky and the underlying UG2, are metre-thick chromitite reefs that together contain well over half of the world's established platinum reserves. The Merensky reef has been mined almost by hand by air-leg[3] miners, working in small scattered groups for well over half a century. These groups drive 18 to 30 m wide faces forward through the thin tabular reefs at ∼17 m per month. Rising labour costs, narrow stopes and powerful low-profile mining machines are leading the current trend towards higher productivity per man shift. In modern mines such as Anglo Platinum's Waterval, mechanized faces can and do advance at 50 to 60 m per month on 180 m fronts. However, washouts, potholes, rolls or faults in the reef that are revealed unexpectedly can bring an advancing section to an abrupt halt. The resulting production ripples adversely affect operations all the way up to the processing plant.

Potholes have drawn significant attention in mechanized mine design because they seriously obstruct production in both the Merensky and the UG2 (Lomberg *et al* 1999). They are local erosive features that interrupt the reef, appear unexpectedly and unpredictably and range in size from 1 m to

[3] A hand-held machine, approximately 90 kg in weight, composed of a steel cylinder and an air operated piston used to support a rock drill.

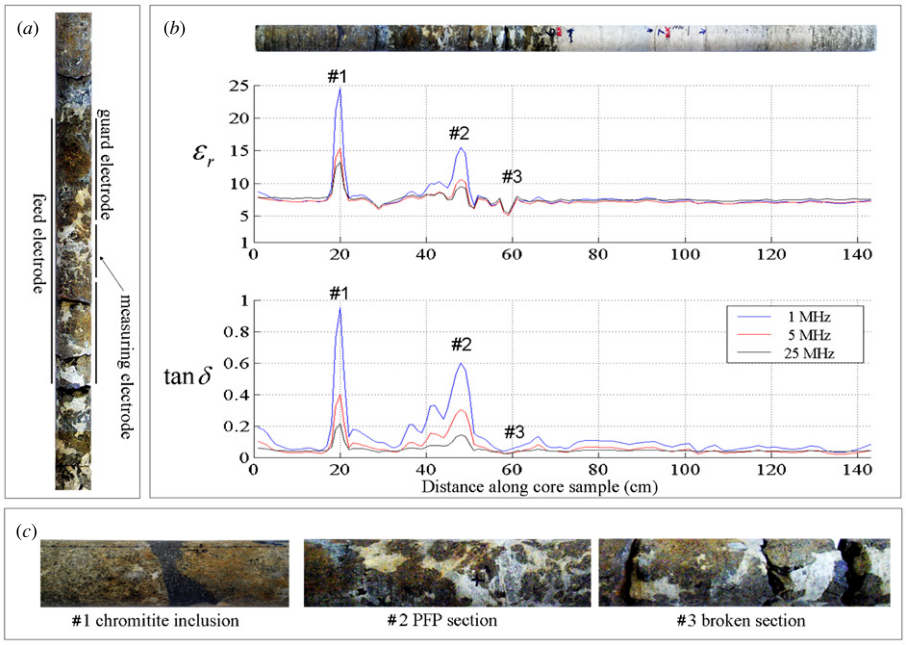

Figure 1. (*a*) The dielectric core sample measurement set-up uses a four-port guarded cylindrical electrode system. (*b*) The mean measured dielectric properties of the entire Bleskop Marker compared to the core above. The properties of the anorthosite and norite sections are fairly homogeneous. (*c*) Pictures of the sections of core sample related to the dielectric property spike. The two spikes are associated with a chromitite stringer and inhomogeneities of the pegmatoidal feldspathic pyroxenite (PFP) section.

greater than 500 m in diameter. These potholes drop from 1 m to 100 m into the foot wall, can have sloping to steep, or even overhanging, margins. They may be slumps or deeply sunken cones, the sides of which may be decorated by shards of chromitite and into which are sucked substantial amounts not only of the hanging wall but also of the adjoining reef. The layers above a deep pothole are deformed, sometimes plastically. They may take the less dramatic but almost equally disruptive form of a simple convergence of foot and hanging walls. Reefs that are thinner than 50 cm are usually deemed unworkable. Washouts are hard to detect remotely because the reef is thin, and horizons in the stratigraphic sequence are perturbed hardly, if at all.

In areas where the overlying Merensky reef has not been mined out, 3D surface seismologists have mapped faults with throws of tens of metres, and detected potholes with diameters of 50 m in the UG2 (Gillot *et al* 2005). There is a growing awareness of the potential of borehole radar as a tool for mapping departures of the UG2 from planarity. Strata hosting the UG2 are almost transparent at ground penetrating radar frequencies of 10–125 MHz. The twin facts that locally uniform interfaces sandwich the UG2, and that it becomes marginal to work just as the UG2 thins towards translucence, can be coupled together (as they are in this paper) both to detect the presence of UG2 thinning and to map the extent of reef reserves that are lost in washouts.

Dielectric properties of the UG2 sequence at borehole radar frequencies

Despite their enormous economic significance, comparatively little is known, petrophysically, about many of the rocks hosting Southern Africa's precious mineral reefs. As a result, it was not obvious that the UG2 reef could be mapped by means of radar remote sensing from boreholes in its footwall when this work commenced in 2001. This dearth provided the incentive for an extensive investigation to yield quantitative, reliable data on the radio frequency properties of the UG2 strata which affect the radiation, propagation, absorption and reflection of electromagnetic pulses from borehole radars (Rütschlin 2005). It was only necessary to measure the macroscopic effective permittivity and conductivity, because the system is essentially non-magnetic.

Representative lengths of diamond drill core were obtained from vertical boreholes through all the rock types in the UG2 sequence near Rustenburg. These included the hanging wall mottled anorthosite (poikilitic pyroxene); the feldspathic pyroxenite hosting the chromitites of the Triplets, Leader and UG2; the pegmatoidal feldspathic pyroxenite at the UG2's base; the footwall norite; and the Bleskop Marker (figure 1) which is found in the UG2 footwall of some areas at Rustenburg.

A four-port guarded cylindrical electrode system was developed (Rütschlin 2005) for use with a Hewlett Packard auto-balancing RF impedance meter to determine accurately the relative permittivity and loss tangent of the various cores in the HF band between 1 and 30 MHz. The use of a cylindrical electrode, shown in figure 1(*a*), through which the core was moved, did away with the need to slice thin samples from the core for use with conventional parallel plate capacitors. By measuring continuous core it was also possible to extract valuable high resolution geophysical information about the properties of thin intrusions and stringers.

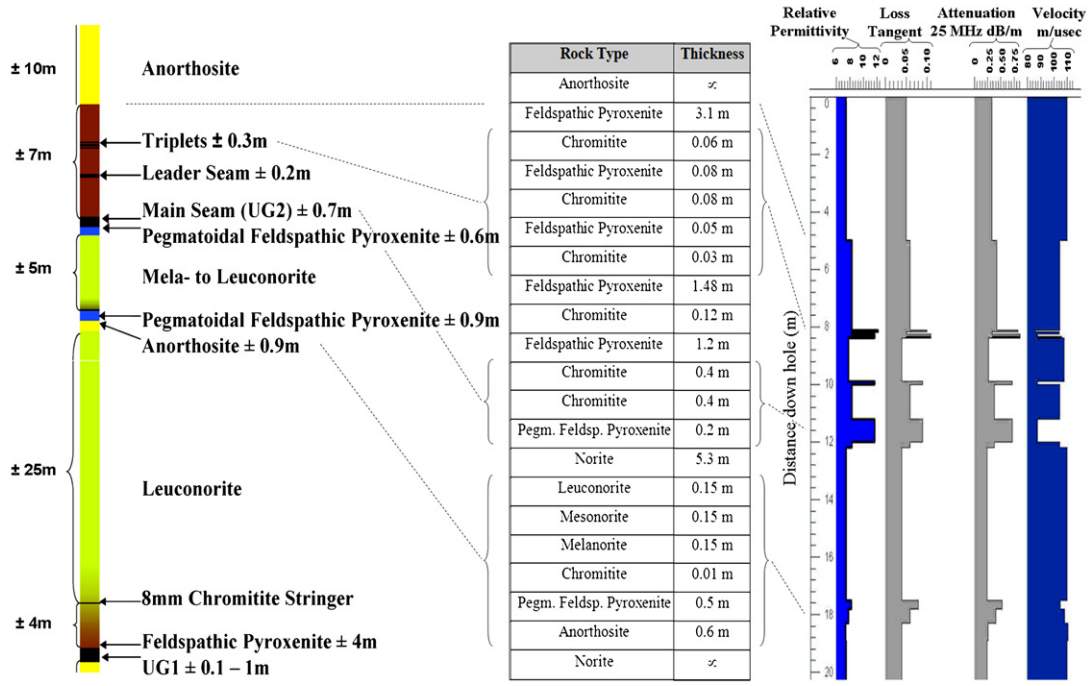

Figure 2. The geological model used for electro-dynamic simulations of the UG2 stratigraphy: left, the common UG2 stratigraphy at Bleskop Platinum Mine; centre, a description of the geological model; and right, plots of continuous logs of the relative permittivity, loss tangent, attenuation, at 25 MHz in dB m^{-1}, and wave velocity in metres/microsecond of the geological model proposed.

The merits of this approach are illustrated in figure 1, where the measured dielectric properties of a 1.5 m length of core through the Bleskop Marker (Vos F 2002, personal communication, 9 September) are presented as a continuous function of distance along the core. The two graphs illustrate spatial variations of the relative permittivity (upper) and the loss tangent (lower) at 1, 5 and 25 MHz which would have been impossible to obtain from sliced samples. Photographic close-ups of the core, associated with the most prominent features in these graphs, lie at the bottom of figure 1.

The core measurements, and the subsequent numerical electro-dynamic simulations (discussed below), strongly supported the feasibility of high resolution borehole radar remote sensing of the UG2 in the HF and VHF band. In particular, it was found that the UG2 footwall is a low loss radar propagation medium; that the UG2 itself is a good radar reflector; and that the propagation and reflection of electromagnetic waves and pulses in the UG2 system could be simulated accurately by representing it as a stack of homogeneous and isotropic horizontal, plane, parallel and smooth sheets, bounded above and below by infinitely thick half-spaces of anorthosite and norite, as shown in figure 2.

The Jonscher formalization (Jonscher 1977, Hollender and Tillard 1998) provides three real constant parameters (n, χ_r and ε_∞) that can be used to analyse propagated and reflected signals, where n is the frequency exponent which characterizes the frequency variation, χ_r is the real part of the electric susceptibility at the reference frequency, and ε_∞ is the limiting high frequency value of the real part of the effective permittivity. For simulation purposes, the Jonscher parameters

Table 1. Representative Jonscher parameters used in the electro-dynamic simulation of borehole radar pulse propagation in the UG2 system.

Rock type	n	χ_r	ε_∞
Anorthosite (UG2 hanging wall)	0.57	0.21	6.86
Feldspathic pyroxenite (UG2 hanging wall)	0.45	0.23	7.59
Chromitite (UG2)	0.40	0.53	10.53
Pegmatoidal feldspathic–pyroxenite (UG2 footwall)	0.49	0.19	7.58
Norite (UG2 footwall)	0.43	0.41	7.51

n, χ_r and ε_∞ of the various rocks of the UG2 system were extracted from the real and imaginary parts of the measured effective relative permittivities (Rütschlin 2005). Some of these are listed in table 1.

Borehole radar reflectivity and transmissivity of the UG2 system

To summarize, since the dip and strike angles of all the strata of the UG2 system are similar, it may be represented locally as a sequence of planar slabs of finite thickness in the absence of local disturbances. The resulting first-order model is depicted in figure 2, where the stratigraphy of practical interest for borehole radar remote sensing extends from the footwall norites below the Bleskop Marker up to hanging wall anorthosites beyond the feldspathic pyroxenite–anorthosite (Px–A) interface.

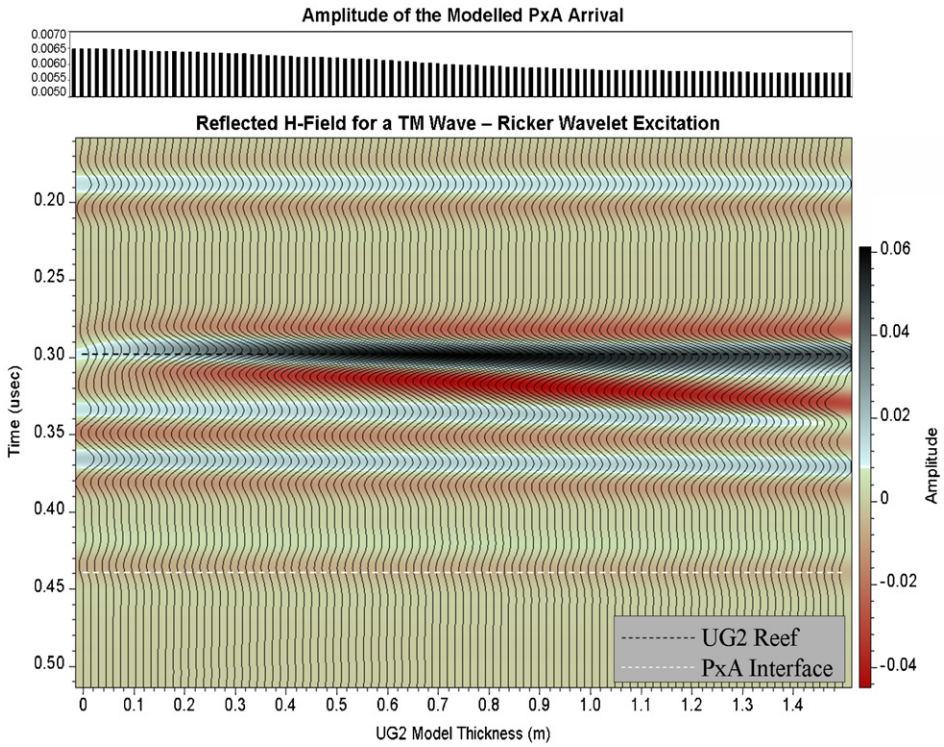

Figure 3. Amplitude of the reflected H-field for normal incidence on the model depicted in figure 2, as the UG2 thickness varies between 0 and 1.5 m, in 15 mm increments. Note that echoes received after 0.3 microseconds correspond to features in the UG2 hanging wall.

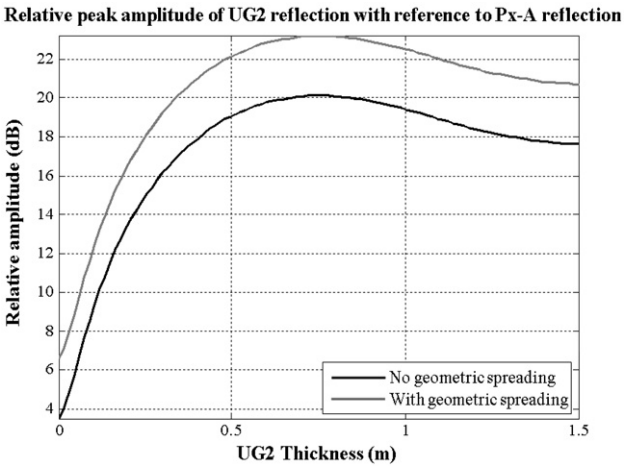

Figure 4. The ratio of reflectivity of UG2 and Px–A plotted against UG2 thickness.

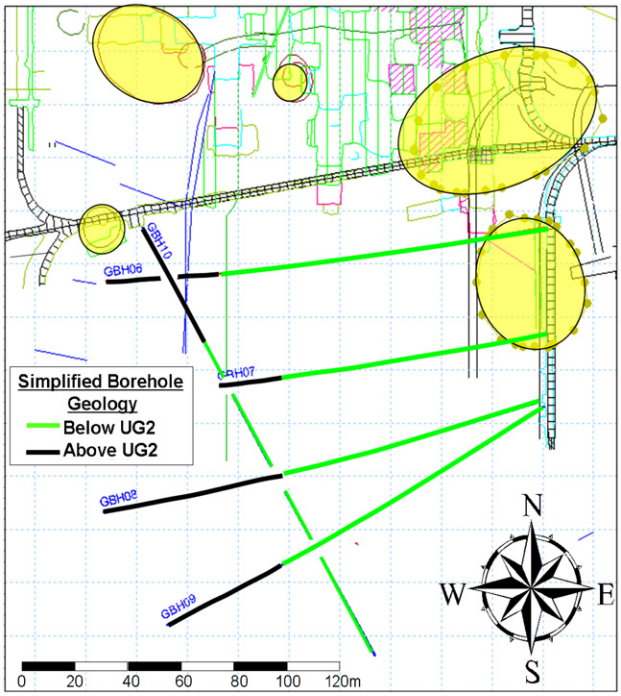

Figure 5. Survey layout for the five boreholes 06, 07, 08, 09 and 10 drilled from UG2 footwall tunnels up through the UG2. Borehole radar data for boreholes 06, 07 and 08 are shown in figure 6.

For the purposes of electro-dynamic simulation the strata were represented by a sequence of homogeneous rocks with known Jonscher parameters. All the parameters were kept constant, except for the thickness of the UG2 which was varied from zero to 1.5 m to study the effect of thickness on its reflectivity and transmissivity. Note that average thickness of the UG2 main reef is about 0.7 m on the Western Limb of the Bushveld Complex near Rustenburg.

The borehole radar, used for the experiments described in the next section, was modelled by a transmit probe which radiated a 20 ns monocycle wavelet (Ricker 1945) and a matched receiver probe (Herselman 2003). In the simulation

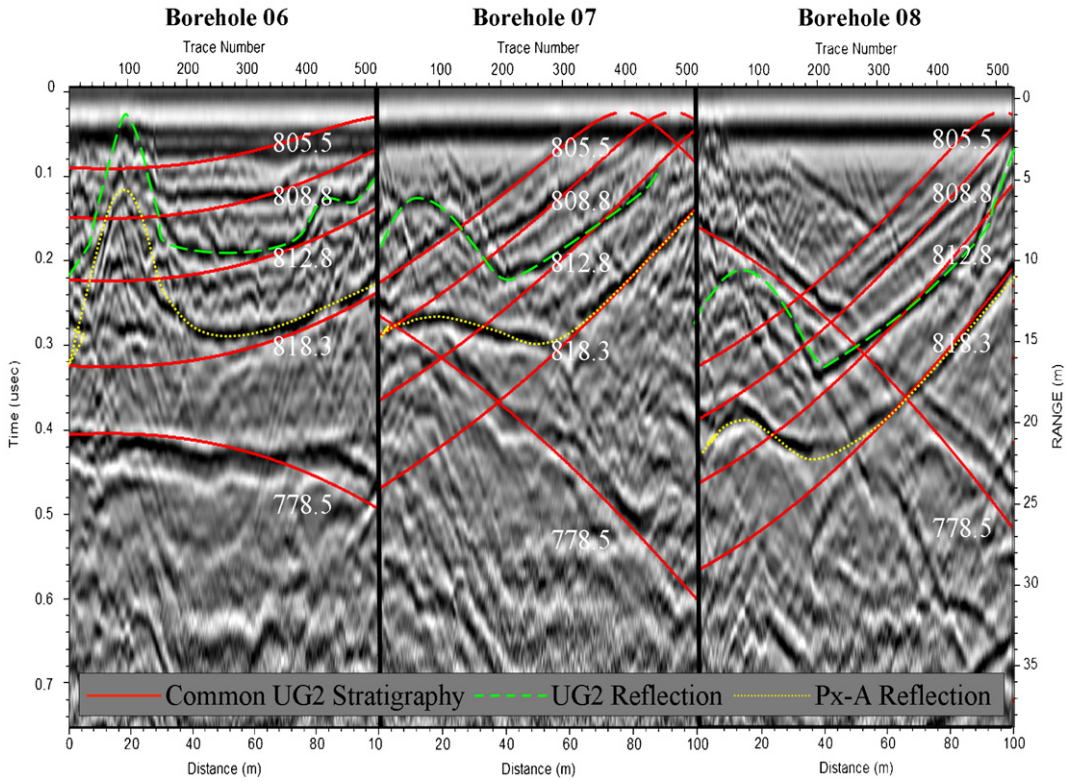

Figure 6. Matching time-sections from boreholes 06, 07, and 08 to a 3D plane-parallel layered model of the common UG2 reef and its surrounding stratigraphy.

they were collocated in a narrow diameter horizontal borehole, 10 m below the Bleskop Marker, in the UG2's footwall norites. Both probes had critically damped (non-resonant) time-domain responses, and electric dipole radiation patterns with their broadside E-fields parallel to the planar interfaces of the strata.

The total magnetic field (infinite series of reflections) at the receiver for a given plane wave excitation $F(\omega)$ was calculated in the spectral domain as

$$H_{1y}^{r} = F(\omega)\tilde{R}_{12}^{\mathrm{TM}}\, \mathrm{e}^{2ik_{1z}d_1}. \qquad (1)$$

Here d_1 represents distance between the radar and the anorthosite base of the Bleskop Marker, and $\tilde{R}_{12}$ is a generalized reflection coefficient that includes the combined effects of reflection from the entire stack above the base of the Bleskop Marker, including multiple bounce reflections (Chew 1990). Equation (1) was derived from the wave equation, for TE polarization, in the ith region of a multilayered system by taking only the upgoing wave and modifying it for TM polarization (Herselman 2003). The appendix describes the reasoning for using a plane wave representation. The resulting time section in figure 3 illustrates how the reflected H-field depends on the thickness of the UG2 reef as it increases from 0 to 1.5 m.

The UG2 reef acts as a Q-spoiled resonator, e.g. Yariv (1985). Its own response tunes as it thickens, capturing much of the limited dynamic range of the grey-scale time section in figure 3 when it passes a thickness of 10 cm. From the point of view of a borehole radar in the footwall, the UG2 shadows reflections from the overhanging pyroxenite–anorthosite (Px–A) interface, 6.5 m (∼0.13 us) above it. The shadowing is effective if the UG2 is thick enough.

Significantly, the economic UG2 mining threshold of ∼60 cm coincides with a knee in the ratio of the reflection amplitudes from the UG2 and the Px–A interface as shown in figure 4.

Case study: UG2 platinum reef remote sensing by borehole radar

Figure 5 shows the survey layout of five boreholes drilled from UG2 footwall tunnels. Figure 6 shows borehole radar profiles that were shot in three of these boreholes. The nearly parallel ∼180 m long AXT (47 mm diameter) boreholes 06, 07 and 08 were drilled in the UG2 footwall norites. They were started near-horizontally and rose slowly towards the UG2 as they were driven westwards from stations spaced by 35 m and 25 m in a horizontal north–south cross-cut beneath the UG2. The intersection of the boreholes with UG2 is shown in figure 5. The profiles shown in figure 6 were filtered and equalized for display purposes using AGC. The horizontal axis of the time-sections in figure 6 shows the distance down the borehole in metres. The left vertical axis shows two-way travel time in microseconds, which can be converted to a range from the borehole, in metres, shown on the right vertical axis.

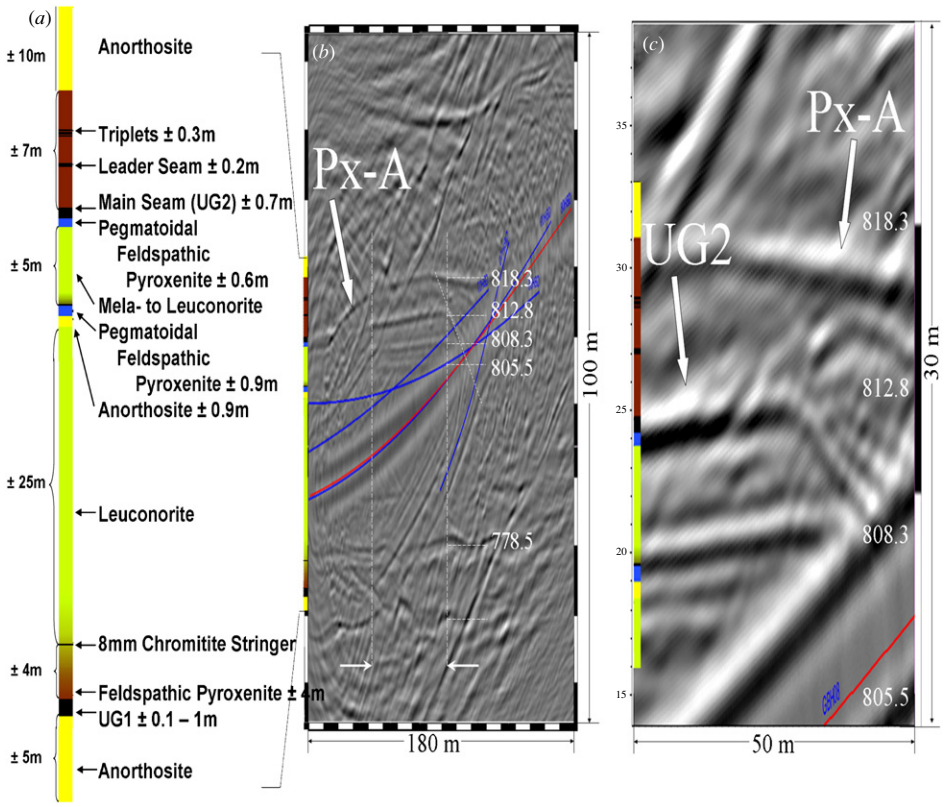

Figure 7. (*a*) The common UG2 stratigraphy at Bleskop Platinum Mine is compared to (*b*) the vertical sagittal plane Huygens–Kirchhoff diffraction stack migration of borehole 08's BHR profile. A mineable corridor of the UG2 is bounded by vertical dashed lines. (*c*) Note that the Px–A echo strengthens as the UG2 echo dims to the right of the mineable corridor.

Smooth curves, superimposed on the time-sections, show the reflection moveout patterns expected from planes parallel to the common UG2 stratigraphy, at elevations of 778.5 m, 805.5 m, 808.8 m, 812.8 m and 818.3 m (measured normal to bedding in local coordinates). The lowest synthetic curve at 778.5 m nominal tracks echoes from the UG1. This lies some 27.5 m beneath the Bleskop Marker (BkM). Echoes from the UG2 at 808.8 m nominal indicate that it lies 3.3 m above the BkM at 805.5 m. The echo four metres higher at 812.8 m nominal is linked to a group of chromitite beds known as the Triplets. And finally, the top echo, tracked at 818.3 m, is associated with the pyroxenite–anorthosite (Px–A) boundary in the UG2's hanging wall.

Dotted curves, superimposed likewise, illustrate the reflection moveout patterns actually observed. The bell shaped swings to the left of the 25 m mark track the descent of the UG2 into a major pothole that lies above the borehole collars. To the right of the 25 m mark, the match of moveout to the stratified time-of-flight model of the previous section is adequate. However, while the UG2's plane may remain intact, the reef may have thinned to the point of being economically un-mineable. Reef thinning should be suspected, particularly if the UG2's echo dims at the same time as echoes strengthen from interfaces in its hanging-wall, such as the overlying Px–A.

In figure 7 we compare the common UG2 stratigraphic column to a Huygens–Kirchhoff diffraction stack migration of borehole 08's BHR profile into a 180 m wide × 100 m high section of the borehole's sagittal plane (the plane linking the hole to its mirror image in the plane of the reef). Vertical dashed lines in the middle diagram indicate a 50 m wide mineable corridor in the UG2, to the left of which both the Px–A echo (at 818.3 m) and the UG2 echo (at 812.8 m) slump into a large pothole. To the right of this mineable corridor, and in the close-up (figure 7(c)), the Px–A echo strengthens as the UG2 echo clearly dims. This is interpreted, in accordance with the foregoing argument, in terms of a thinning of the reef below the 50 cm mining cut-off.

Conclusions

The fact that borehole radar remote sensing indicates a fairly narrow mineable corridor, bounded by a large deep pothole to the east, and by slumping, thinning and shearing to the west, is of obvious immediate concern to local mining engineers. But what may well be of more general and lasting interest is the observation that the Px–A boundary can be mapped through mineable UG2, right across the corridor.

Thick UG2 is not transparent, but it certainly is translucent. The demonstration of a footwall borehole radar's ability to map structures in the UG2's immediate hanging wall bears indirectly on mine safety, for roof-bolts must be long enough driven through some of these drifting structures.

Appendix. Plane wave representation of radiation from spatially finite sources

Since EM waves are generated by spatially finite sources, the wave fronts are non-planar. However, just as finite length time-domain pulses can be represented by an infinite ω-domain Fourier spectrum, so can the radiation patterns of coherent, finite sources be represented by their plane wave spectrum (Chew 1990). Under a number of conditions the approximation of a wave by a single plane wave (spectral domain impulse) with defined amplitude at a given geometrical location and unique directions of increasing phase and decreasing amplitude (King *et al* 1992) yields results that are essentially identical to the asymptotic full-wave solution.

In the classic Sommerfeld problem where the radiation field of an electro-dynamic dipole radiating above a lossy dielectric has to be calculated, the asymptotic solution for a dipole sufficiently high above the ground is equal to the vector sum of the direct spherical wave and a reflected spherical wave that originates at the source's image point below the surface with a reflection coefficient equal to the plane wave reflection coefficient for the given geometry (incidence angle) (Ishimaru 1991).

This theory can be expanded to a multilayered system (Chew 1990). With their Jonscher parameters known, the plane wave reflection coefficients for the different layer interfaces can be calculated, and therefore the reflected wave due to a borehole radar illuminating a sequence of horizontal, planar rock layers provided the transmitter and receiver are sufficiently distant (in wavelengths) from the first interface.

References

Cawthorn R G 1999 Platinum-group element mineralization in the Bushveld Complex—a critical reassessment of geochemical models *South Afr. J. Geol.* **102** 268–81

Chew W C 1990 *Waves and Fields in Inhomogeneous Media* (New York: Van Nostrand Reinhold)

Gillot E, Gibson M, Verneau D and Laroche S 2005 Application of high-resolution 3D seismic to mine planning in shallow platinum mines *First Break* **23** 59–64

Herselman P Le R 2003 Borehole radar system analysis in stratified geological systems applied to imaging of platiniferous reefs in the Bushveld Igneous Complex *PhD Thesis* University of Stellenbosch, South Africa

Hollender F and Tillard S 1998 Modelling ground-penetrating radar wave propagation and reflection with the Jonscher parameterization *Geophysics* **63** 1933–42

Ishimaru A 1991 *Electromagnetic Wave Propagation, Radiation and Scattering* (Englewood Cliffs, NJ: Prentice-Hall)

Jonscher A K 1977 The universal dielectric response *Nature* **267** 673–9

King R W P, Owens M and Wu T T 1992 *Lateral Electromagnetic Waves* (New York: Springer)

Lomberg K G, Martin E S, Patterson M A and Venter J E 1999 The morphology of potholes in the UG2 chromitite layer and Merensky Reef (pothole reef facies) at Union Section, Rustenburg Platinum Mines *South Afr. J. Geol.* **102** 209–20

Ricker N 1945 The computation of output disturbances from amplifiers for true wavelet inputs *Geophysics* **10** 207–20

Rütschlin M 2005 The non-destructive measurement of the radio frequency properties of hard rock borehole cores *PhD Thesis* University of Stellenbosch, South Africa

Yariv A 1985 *Optical Electronics* (New York: Rinehart and Winston)